Physical Deposition Profile Based Toolpath Generation and Optimization for Additive Volume Building in Hybrid Additive Manufacturing

Zhen Hong, Zhiping Wang, Sihao Deng, Yicha Zhang, Alain Bernard

Physical Deposition Profile Based Toolpath Generation and Optimization for Additive Volume Building in Hybrid Additive Manufacturing

Zhen Hong*, Zhiping Wang*, Sihao Deng†, Yicha Zhang#, Alain Bernard*

*Ecole Centrale de Nantes, LS2N, CNRS UMR 6004, Nantes, France
†UTBM – Université de Technologie Belfort-Montbéliard, ICB-PMDM, CNRS UMR 6303, Sevenans, France
#UTBM – Université de Technologie Belfort-Montbéliard, ICB-COMM, CNRS UMR 6303, Sevenans, France

Abstract

In hybrid additive manufacturing (HAM), toolpaths affect the volume building and removing during the sequential or iterative hybrid processing since they control the deposition nozzle or cutting tools. In sequential hybrid additive manufacturing, toolpaths for additive manufacturing module define the volume directly determines of the shape accuracy and volume building time. In this paper, we report a new toolpath generation and optimization method for a developing cold spraying - based HAM process's additive processing module. This method adopts a valid physical deposition profile to set scanning parameters and then applies an evolutionary optimization algorithm to minimize the total scanning length for building a set of ordered disconnected volumes on a predefined base. The propose method is illustrated by a complex tree shape model and validated by three selected numerical examples. It has potential to help save spraying raw materials and time as well as improve shape accuracy.

Key words: toolpath optimization, profile-based sweep, Hybrid Additive Manufacturing (HAM).

1. Introduction

During the past more than three decades, additive manufacturing (AM) becomes more and more essential for functional manufacturing as the process and material development [1], because of its capacity to manufacture parts with complex surface and internal geometries by adding layers of materials without the use of tooling or fixtures enables [2], as well as the freedom to design, mass personalization, less shipping parts and warehouse storage, and less waste and energy consumption [3][4][5][6]. Even though AM has many advantages, compared with traditional processing technologies, limitations still exist, such as poorer dimensional accuracy and surface quality [7][8], limited materials and relatively long printing time for some applications [9], especially for metallic AM processes. Therefore, only AM being employed, it is probably costly

and not easy to guarantee high accuracy and feasibility. On the contrary, traditional manufacturing processes like CNC, have many advantages, such as high speed and high quality of finish surface, which can greatly compensate the shortcomings of AM [9]. Therefore, the combination of additive and traditional manufacturing processes is considered as a promising solution to compensate the limitations of both AM and traditional processes by taking advantage of the strength of both AM and traditional processes [10][11]. As a consequence, the combination brings new opportunities for various applications [12] and is increasingly employed for producing or remanufacturing functional parts [8] [13][14][15]. For the existing research of hybrid additive manufacturing, there are sequential processes and iterative processes [16]. In this paper, The HAM is a sequential process, specifically, cold spray with CNC.

Although the hybridization idea of the two types of processes seems simple, the real operation for process combination becomes more difficult since both of the existing constraints of AM and NAM processes are introduced and couple with each other. Therefore, the process planning for HAM is critical for the implementation of process combination. Some researchers noticed the importance of this and had already conducted a few investigations as reviewed in [17] . However, there are still a plenty of problems not well solved or even touched. such as selection on candidate processes for HAM, manufacturability analysis for HAM, estimate the process from zero or an existing volume, the generation of the existing volume, sequence planning, toolpath planning, etc.

This research focuses on the question of toolpath generation in the AM module for multi-axis HAM, based on Cold Spray (CS) with CNC. For the existing research of toolpath planning for AM, there are some limitations such as, no consideration of the real deposition profile, less study on the step length of declination angles, using rastering/zigzag, etc. To solve this problem, this paper introduces a geometric computational method to generate an optimal toolpath angle for each layer, with the consideration of toolpath length, but it is illustrated mainly for AM.

The remained structure of this article is as follows: section 2 is about the existing researches of tool path planning; in section 3, the proposed method is implemented and the case study is operated in the following section. The last section is about the conclusions of this research and the perspective of future work.

2. Related work

This research focuses on process planning for sequential multi-axis HAM and the CSHAM (Cold Spray-based Hybrid Additive Manufacturing) platform is in development at UTBM, which is a modular HAM robotic platform, where robots are used as connections to link different existing processing modules/machines. Therefore, there is no need to integrate and modify the existing machines, and it is more flexible, reconfigurable, sustainable, etc. In the CSAM platform, the CS

gun is fixed, and the robot catches the substrate to fix the initial volume (an existing volume to deposit material onto and become one part of the final component). In this article we focus on the toolpath for AM module in CSHAM, which similar with other types of AM, but a little different, because the CS gun cannot stop. Therefore, the length of the toolpath is important in this research.

Since toolpath planning is very important for AM, there exist much research as mentioned above. Moreover, for multi-axis AM process, the toolpath can be 3D curve paths [18]. However, most HAM systems still use planar scanning in the AM processes. And toolpath planning for AM can be divided into two components: interior and exterior path planning and varies due to different AM technologies [19]. In addition, the process of filling in the interior of the layer is accomplished by means of path planning, while the external is usually by removing materials [19]. Various types of toolpath patterns from milling can be introduced into AM, such as rastering similar with zigzag, contours, spirals, and some other filling patterns [20]. And the popular types are as follows in Figure 1.

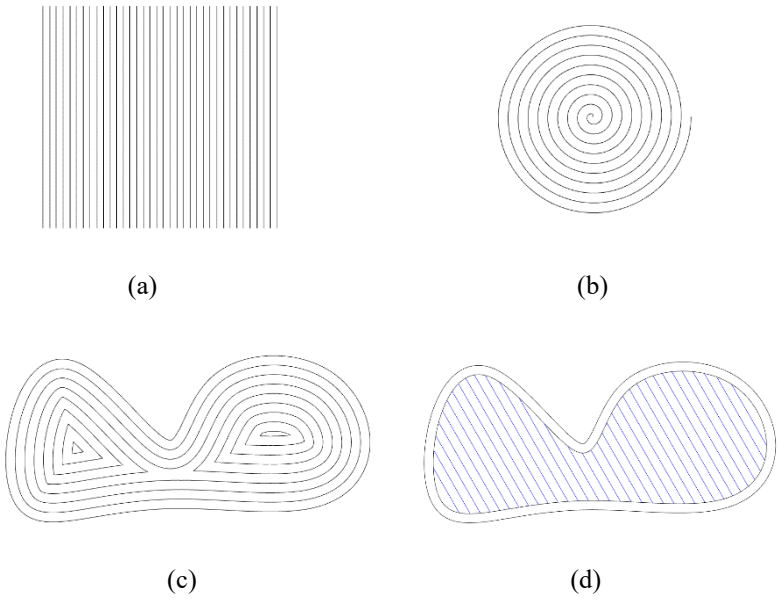

Figure 1 - Typical trajectories: rastering, spiral, offset, and combined type.

One crucial issue to be addressed relates to offset problems along the trajectories. The problems of offset [21] are divided into three types: void type I occurs when the area to be filled is too large for a single pass, but not large enough for another parallel offset path; void type II occurs when corner geometry has too sharp of an angle, depending on specific process parameters such as laser spot size; void type III will occur if the offsetting algorithm generates more than one loop allowing a void between the separated loops [21]. The spiral path has similar void with offset method and a new spiral path is generated that has no sharp corners. So one method to improve the

problem is proposed and the brief procedures are as follows [22]: (1) Obtain MAT (medial axis transform) of original 2D cross-sections, (2) Re-parameterize the skeleton by arc length, (3) Solve the above optimization problem, (4) Compute spiral paths from the medial axis and the optimized radius function. The zigzag path is also very generally used. Liou et al. developed a hybrid manufacturing process with coverage toolpath planning, zigzag with interlaced direction [23].

For a continuous 5-axis laser cladding process, the experiments to study different toolpath strategies and to arrive at an optimal toolpath consider quantitative criteria such as the deposition rate, the wetting angle and the height and width clad tracks [24]. A configuration space approach to enable toolpath planning in a full three-dimensional space allows movements beyond planar slices [25]. The researchers in [25] change to the 2.5D paradigm by using a configuration space approach to enable toolpath planning in a full three-dimensional space, allowing movements beyond planar slices in the point-based AM systems which have many features in common with CNC milling machines. Moreover, medial axis transformation was used for adaptive path planning of wire-feed additive manufacturing [26].

To reduce build time, a concurrent toolpath planning algorithm generates collision-free multi-toolpaths to control the tools that deposit materials concurrently [27]. A mixed and adaptive toolpath generation algorithm has been then developed, aiming to optimize both the surface quality and fabrication efficiency in AM [28]. For further improvement on fabrication quality, a toolpath adjustment is employed on the original toolpaths [29]. A mixed and adaptive toolpath generation algorithm is proposed to generate contour toolpaths for the boundary of each layer to make sure the surface quality, and zigzag toolpaths for the internal area of the layer to reduce build time. Moreover, the best slope degree of zigzag toolpaths is selected to further minimize the build time [28]. Similarly, another research is also on the inclinations with very few angles [30]. Therefore, there are limitations for the step length of scanning angles.

Table 1 The limitations of existing method on toolpath planning.

The method	The limitations	Ref.
Contour	Three types of voids	[21]
spiral path	Spiral path has similar voids with offset method	[22]
Contour and zigzag	Only 6 different angles	[28]
Contour and zigzag	Only 8 different angles	[30]

In conclusion, there are still some limitations of toolpath planning, illustrated in table 1, and specially, the existing toolpath generation method did not consider many slope angles for optimization and real physical deposition profile. Moreover, there is no consideration of toolpath configuration for each layer (scanning type, angle, speed, energy, etc.). So, it is necessary to propose a method for toolpath generation and optimization to solve the above-mentioned limitations.

Given the limitations of the existing toolpath planning for AM. In our research, a potential method is proposed and the toolpath generation combines different toolpath types, the contour and rastering in this paper, and the rastering angles are optimized considering the total length of toolpath. The details of this methods are descripted in the next section.

3. Methodology

3.1. The global introduction of the proposed method

From the existing methods in the literature mentioned in section 2 for toolpath generation, for planar toolpath, combining different toolpath types can lead to good quality with less fabrication time and the proposed method is illustrated in Figure 2.

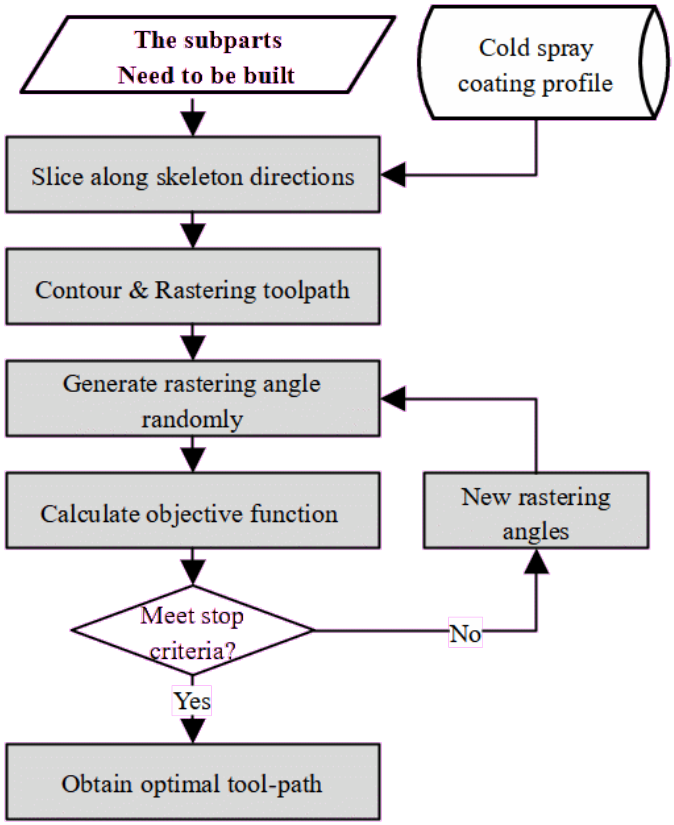

Figure 2 - The proposed method for toolpath optimization.

From the existing methods as abovementioned, we can see that the limitation of existing methods for toolpath planning. In this research, only contour (for the two passes outside) and

rastering (inside) are employed and the total toolpath length is optimized by varying the rastering angles with a small step length, 0.1 degree, by Particle Swarm Optimization algorithm (PSO).

3.2. The introduction of the physical profile of CS

In this research, for demonstration, we take the cold-spay-based HAM process for demonstration. The toolpath generation is based on coating profile proposed by Hongjian Wu et al. [31]. The deposition is a three-dimensional geometric model based on Gaussian Distribution as well as the 2D cross-section profile, shown in Figure 3.

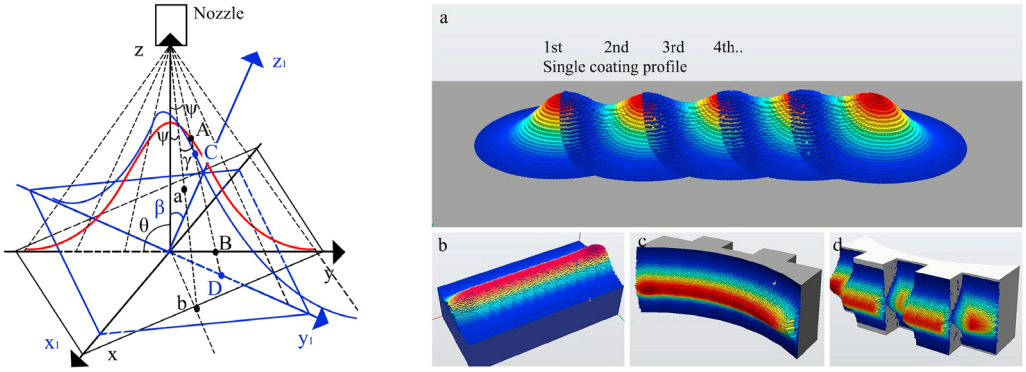

(1) (2)

Figure 3 – The schematic of single coating profile model and different kind of overlaps on various surfaces [31].

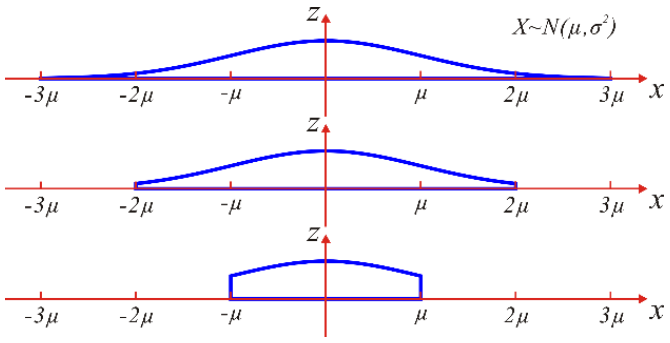

Figure 4 – The Gaussian distribution in GH.

In Figure 3 (1), it shows the schematic of single coating profile model on X-Y plane (red line) and X1-Y1 plane (blue line). θ and β are the spray angle on X-Y plane and X1-Y1 plane

respectively. a is the angle between Z axis and Z1 axis. ψ is the deflection angle (the angle between Z axis and ab line, as well as AB line). γ is the angle between ab line and AB line. Figure 3 (2) (a) shows discrete single coating profile with overlaps, (b) continuous single coating profile on a flat surface, (c) continuous single coating profile on a curved surface, (d) continuous single coating profile on a complex surface. The Gaussian distribution profile [32] is generated in GH (Grasshopper) as in Figure 4. The section of 2μ is used as a reference to define the layer thickness and hatching space.

3.3. The PSO optimization algorithm

Since GA (Genetic Algorithm) is very slow for iterations, the Particle Swarm Optimization algorithm (PSO) is adopted for searching optimal initial volume. The flow chart of PSO is illustrated in Figure 5.

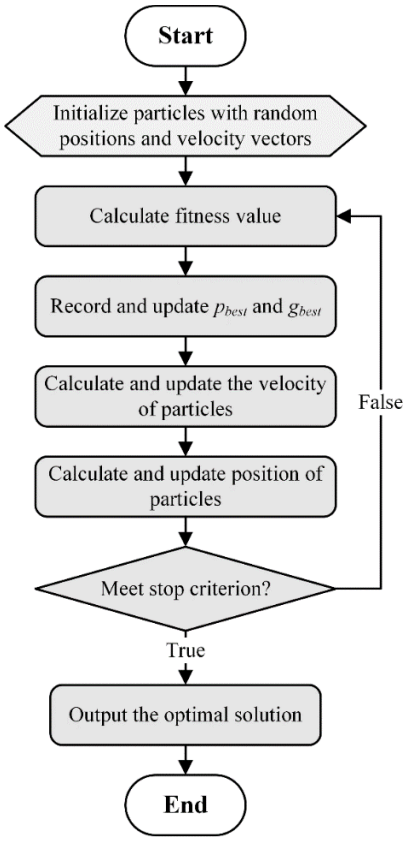

Figure 5 - The basic steps of PSO.

The PSO algorithm is a sub-field of Computational Intelligence. It belongs to swarm intelligence and collective intelligence and has both ties with artificial life and evolutionary computation. PSO is a type of biological system inspired by bird flocking and fish schooling. Its

simulation was motivated by the need to model 'human social behavior' and the collective behaviors of individuals interacting with each other and their environment from the optimization process [33]. One plugin called Silvereye is introduced by visual programming in Grasshopper for Rhino3D modeling environment [34].

The slicing process is operated along the skeleton (the medial axis of the CAD model) direction evenly. The sliced layers with a fixed thickness referred from the experimental results of cold spray, the Gaussian distribution [31]. The layers will be filled by the combined toolpath, i.e., contour with rastering, and the rastering with different angles inside. The whole toolpath length of one subpart is adopted as the objective to optimize the angle.

The idea is to use the result of adopted experimental deposition as cross-section profile to sweep along the generated toolpath to form 3D volume for the AM processing. For each layer, the process starts from outside to inside and the first two passes are contour trajectories to guarantee the accuracy. The objective is to minimize the length of the total toolpaths. The raster angles are optimized for each layer of every subpart which need to be built by adding materials and the step length of 0.1 degree for rastering is chosen based on the limitation of robot move precision. The following section introduces a PSO implementation for toolpath length optimization. For the encoding, each layer is one gene, so one chromosome is shown in Table 2.

Table 2. The encoding of different layers of one subpart.

Layer	1	2	3	4	5	6	7	....	...	n
Angle	α_1	α_2	α_3	α_4	α_5	α_6	α_7	....	...	α_n

In the optimization process, the objective function is the total toolpath length shown in equation (1):

$$\text{Min: } L = \sum_{i=1}^{n} l_i^{\alpha_j} \tag{1}$$

$$\alpha \in [0°, 180°)$$

where, L is the total length of all toolpaths; α is the rastering angle and $l_i^{\alpha_j}$ is ith layer's toolpath length with a rastering filling angle of α_j.

3.4. **The illustrative example**

To illustrate the method, a tree structure CAD model is employed, shown in Figure 6 (a), the volume (called the initial volume) in Figure 6 (c) is obtained by traditional processes, and the remaining volumes that need to be manufactured by depositing materials onto the initial volume

are shown in Figure 6 (d), which is decomposed into different subparts (the decomposition process is out the scope of this paper), based on the skeleton of the tree model, shown in Figure 6 (b).

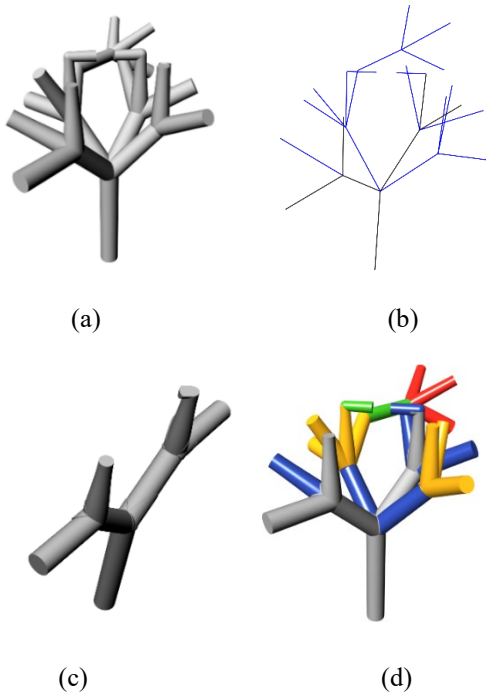

Figure 6 – (a). The tree model; (b). The skeleton of the tree; (c). The initial volume; (d). The remaining volumes (except the initial volume in grey).

Table 2. The parameters set in Silvereye.

Parameter	Swarm size	Iteration	Max. Velocity
Value	20	1000	0.2

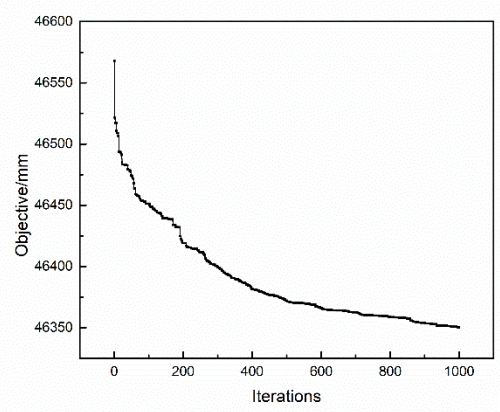

Figure 7 - The shortest toolpath length of each iteration.

(a) (b) (c)

Figure 8 - (a). The selected subpart; (b), (c). One layer to show the details of toolpath.

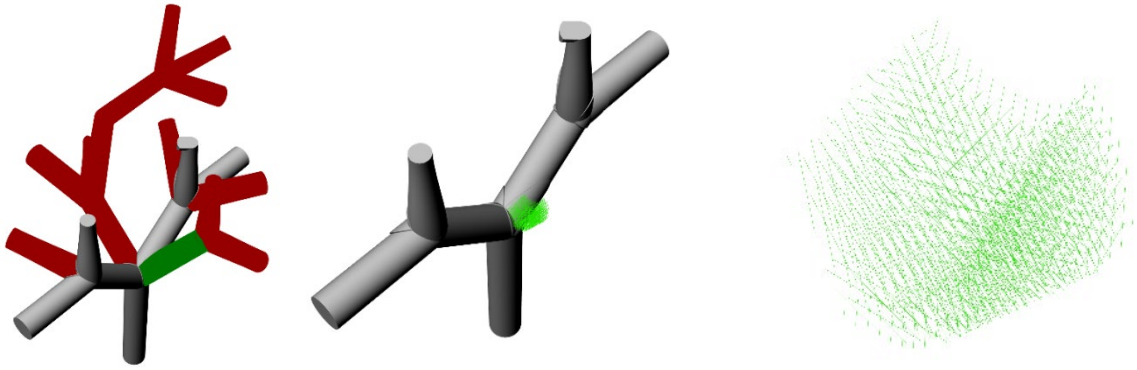

(a) (b) (c)

Figure 9 - (a). The toolpath of all the subparts that have no collisions; (b), (c). Several layers of one selected subpart.

For the tree model, one subpart is chosen for demonstration, illustrated in Figure 8 (a). After the calculation of 1000 iterations, the corresponding shortest length of this subpart of tree model for each iteration is shown in Figure 7. One layer is selected to show the details of toolpath, shown in Figure 8. (b), (c). Since the layer with the same cross-section, the angles are the same (the white cylinder), shown in Figure 8. (b). All of the subparts with no collisions (the collision test is out of the scope of this article) have obtained their corresponding optimal toolpath by optimizing the rastering angles. The final result for the whole tree is illustrated in Figure 9 (a) with the details of local toolpath of one selected subpart in Figure 9 (b), (c).

In conclusion, in this research, the method has been proposed to improve toolpath planning and it is implemented with one complex tree model. In the following section, three case studies are operated to show the application of the proposed method.

4. Case study

Three examples are adopted at different complexity levels to test the proposed method. The first model is simple and the second one is selected from a published paper [35] ,which is designed for CS process. The third one is a part of the plane, which is complex and challenging to manufacture.

4.1 Case 1

The first case is a simple model shown in Figure 10 (a), and the grey part of Figure 10 (c) is the initial volume of case 1, which will be manufactured by traditional process. The green volumes are the remaining volumes that will be obtained by CS, and these remaining volumes will be decomposed into subparts according to the skeleton of case 1, but the details are beyond the scope of this paper.

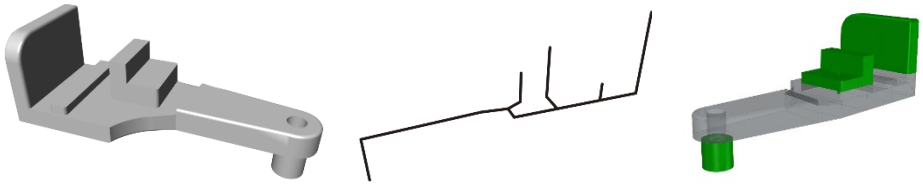

(a) (b) (c)

Figure 10 – (a). The CAD model of Case 1; (b). The skeleton of case 1; (c). The initial volume (in grey) and remaining volumes (in green).

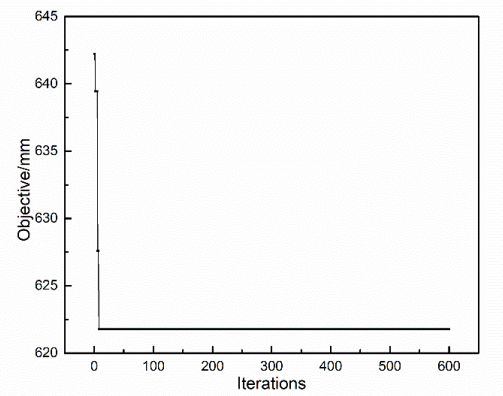

Figure 11 – The shortest toolpath length of each iteration of the selected subpart in case 1.

The evolutionary optimization algorithm PSO is adopted the same as for the tree model, and the calculation is also operated in the Silvereye plugin. The parameters are set the same as for the tree model, except the iteration number is 600.

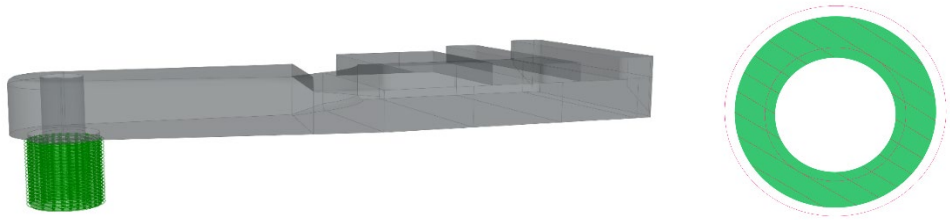

(a) (b)

Figure 12 – (a). The toolpath of one subpart; (b). The details of one layer of the selected subpart.

Because the cross-sections are even for the subparts, these angles are assumed the same for all layers of the whole subpart, shown in Figure 12. For all the remaining subparts, the process is similar, and the optimal toolpath for all the subparts is shown in Figure 13.

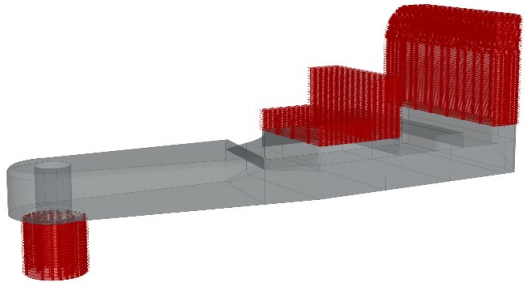

Figure 13 - The toolpath of all the subparts.

4.2 Case 2

The second model is from the existing research, a bracket manufactured with a cold spray process [35] and its CAD model is shown in Figure 14 (a). The whole model is built from scratch in their method, which needs an extensive support structure and causes many wasted materials. In

our method, the process starts from an existing volume, called the initial volume. The initial volume is shown in Figure 14 (b), and the remaining volumes are in Figure 14 (c).

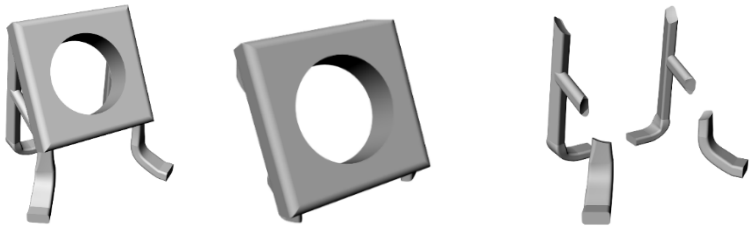

(a) (b) (c)

Figure 14 – (a). The CAD model of case 2; (b). The initial volume; (c). The remaining volumes to deposit material onto the initial volume.

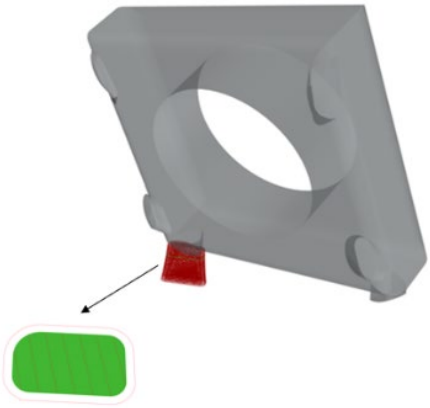

Figure 15 - The toolpath of one subpart with the details of one of its layers.

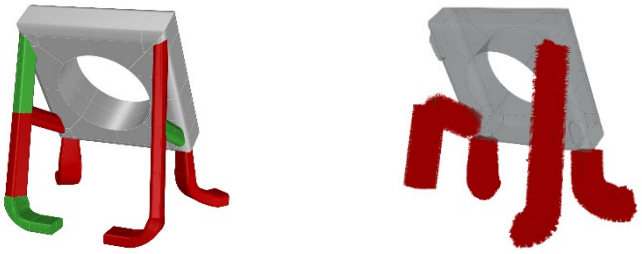

(a) (b)

Figure 16 – (a). The subparts need collisions (in green); (b). The toolpath of all the subparts without collisions in case 2.

One subpart of case 2 is chosen, and one of its layers is selected to show the details of optimal result, illustrated in Figure 15. Moreover, in this case, three green subparts, shown in Figure 16 (a), have collisions. Therefore, these three subparts are not considered for optimizing the toolpath, so only other subparts are manufactured by our method. The optimal toolpath of all of these subparts is illustrated in Figure 16 (b).

4.3 Case 3

The third case shown in Figure 17 is more complex than the previous two cases. And its CAD model is shown in Figure 17 (a), and the initial volume is in Figure 17 (b), as well as the remaining volumes are in Figure 17 (c).

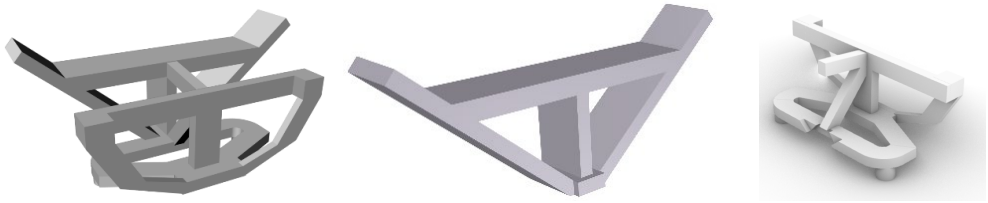

(a) (b) (c)

Figure 17 - (a). The CAD model of case 3; (b). The initial volume; (c). The remaining volumes to deposit material onto the initial volume.

One subpart shown in Figure 18 is taken as an example to illustrate the optimized result. All of the subparts with no collisions have obtained their corresponding optimal toolpath by optimizing the rastering angles shown in Figure 19 (a). All the subparts which have collisions are the red ones shown in Figure 19 (b).

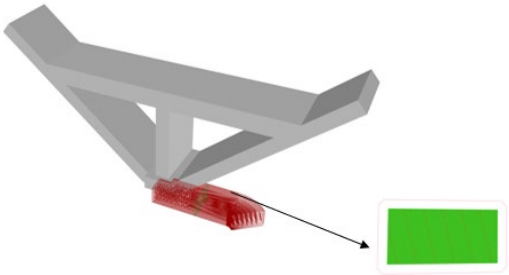

Figure 18 - One subpart and one of its layers.

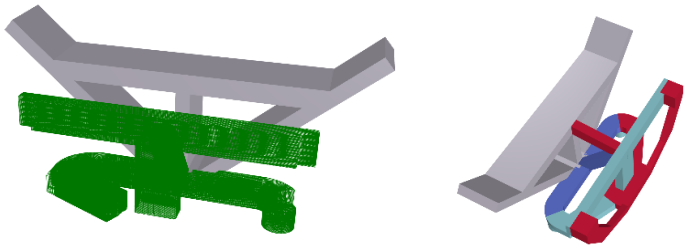

(a) (b)

Figure 19 - (a). The toolpath of all subparts which do not have collisions in case 3; (b). The subparts that have collisions (in red)

5. Conclusions and Perspectives

In this research, a new method is improved to optimize toolpath planning considering the rastering with a small step length, 0.1 degree, for each layer. This method uses combined toolpath types, i.e., the combination of different toolpath types, and the boundary of each layer is contour, while the rastering is used to fill the inside area. The whole toolpath length is considered as a main criterion to find the optimized rastering angles for each layer in our research.

However, this toolpath planning method only considers planar slicing perpendicular to the skeleton branches. In addition, since the slicing process greatly influence the toolpath planning, and in our research, the slicing is multi-direction based on the skeleton (medial axis) of the CAD model, but uniform and planar. Therefore, nonplanar layers will be taken into account in the future for multi-axis process. Furthermore, we do not consider the complexity and sub-regions of each layer, so some research needs to be operated on both complex and too large cross-sections. Moreover, for large cross sections, the decomposition of cross-sections may be necessary to use more than one cutting tools or deposition nozzles in parallel to save time. It is also essential to consider the collision and iteration with traditional process like CNC/laser cutting (SM process).

Reference

[1] J. K. T. Wohlers, W. Associates, R.I. Campbell, O. Diegel, R. Huff, “Wohlers Report 2020: 3D Printing and Additive Manufacturing State of the Industry.” Wohlers Associates2020, 2020.

[2] Zhang, Y., Wang, Z., Zhang, Y., Gomes, S., & Bernard, A. (2020). Bio-inspired generative design for support structure generation and optimization in Additive Manufacturing (AM). CIRP Annals, 69(1), 117-120.

[3] Thompson, M. K., Moroni, G., Vaneker, T., Fadel, G., Campbell, R. I., Gibson, I., ... & Martina, F. (2016). Design for Additive Manufacturing: Trends, opportunities,

considerations, and constraints. CIRP annals, 65(2), 737-760.

[4] Bandyopadhyay, A., Gualtieri, T. P., & Bose, S. (2015). Global engineering and additive manufacturing. Additive Manufacturing, 1, 9-11.

[5] Gao, W., Zhang, Y., Ramanujan, D., Ramani, K., Chen, Y., Williams, C. B., ... & Zavattieri, P. D. (2015). The status, challenges, and future of additive manufacturing in engineering. Computer-Aided Design, 69, 65-89.

[6] Gibson, I., Rosen, D., Stucker, B., & Khorasani, M. (2014). Additive manufacturing technologies (Vol. 17, p. 195). New York: Springer. I. G. David Rosen and B. Stucker, *Additive Manufacturing Technologies*. 2015.

[7] Vayre, B., Vignat, F., & Villeneuve, F. (2012). Metallic additive manufacturing: state-of-the-art review and prospects. Mechanics & Industry, 13(2), 89-96.

[8] Paris, H., & Mandil, G. (2017). Process planning for combined additive and subtractive manufacturing technologies in a remanufacturing context. Journal of Manufacturing Systems, 44, 243-254.

[9] Ramaswami, K. (1997). Process planning for shape deposition manufacturing (Doctoral dissertation, stanford university).

[10] Flynn, J. M., Shokrani, A., Newman, S. T., & Dhokia, V. (2016). Hybrid additive and subtractive machine tools–Research and industrial developments. International Journal of Machine Tools and Manufacture, 101, 79-101.

[11] Karunakaran, K. P., Suryakumar, S., Pushpa, V., & Akula, S. (2010). Low cost integration of additive and subtractive processes for hybrid layered manufacturing. Robotics and Computer-Integrated Manufacturing, 26(5), 490-499.

[12] Zhu, Z., Dhokia, V. G., Nassehi, A., & Newman, S. T. (2013). A review of hybrid manufacturing processes–state of the art and future perspectives. International Journal of Computer Integrated Manufacturing, 26(7), 596-615.

[13] Ren, L., Eiamsa-ard, K., Ruan, J., & Liou, F. (2007, January). Part repairing using a hybrid manufacturing system. In International Manufacturing Science and Engineering Conference (Vol. 42908, pp. 1-8).

[14] Jones, J. B., McNutt, P., Tosi, R., Perry, C., & Wimpenny, D. I. (2012). Remanufacture of turbine blades by laser cladding, machining and in-process scanning in a single machine.

[15] Paris, H., & Mandil, G. (2018). Extracting features for manufacture of parts from existing components based on combining additive and subtractive technologies. International Journal on Interactive Design and Manufacturing (IJIDeM), 12(2), 525-536.

[16] Patterson, A. E., & Allison, J. T. (2018, January). Manufacturability constraint formulation for design under hybrid additive-subtractive manufacturing. In ASME 2018 International Design Engineering Technical Conferences and Computers and Information in Engineering Conference. American Society of Mechanical Engineers Digital Collection.

[17] Nassehi, A., Newman, S., Dhokia, V., Zhu, Z., & Asrai, R. I. (2012). Using formal methods to model hybrid manufacturing processes. In Enabling Manufacturing Competitiveness and Economic Sustainability (pp. 52-56). Springer, Berlin, Heidelberg.

[18] Xie, F., Bi, D., & Tang, K. (2020). A potential field based multi-axis printing path generation algorithm. International Journal of Computer Integrated Manufacturing, 33(12), 1277-1299.

[19] Kulkarni, P., Marsan, A., & Dutta, D. (2000). A review of process planning techniques in layered manufacturing. Rapid prototyping journal.

[20] Jin, Y. A., He, Y., Fu, J. Z., Gan, W. F., & Lin, Z. W. (2014). Optimization of tool-path generation for material extrusion-based additive manufacturing technology. Additive manufacturing, 1, 32-47.

[21] Ren, L., Ruan, J., Eiamsa-ard, K., & Liou, F. (2007, January). Adaptive deposition coverage toolpath planning for metal deposition process. In International Design Engineering Technical Conferences and Computers and Information in Engineering Conference (Vol. 48078, pp. 413-419).

[22] Kao, J. H., & Prinz, F. B. (1998, September). Optimal motion planning for deposition in layered manufacturing. In Proceedings of DETC (Vol. 98, pp. 13-16).

[23] Ren, L., Eiamsa-ard, K., Ruan, J., & Liou, F. (2007, January). Part repairing using a hybrid manufacturing system. In International Manufacturing Science and Engineering Conference (Vol. 42908, pp. 1-8).

[24] Calleja, A., Tabernero, I., Fernández, A., Celaya, A., Lamikiz, A., & De Lacalle, L. L. (2014). Improvement of strategies and parameters for multi-axis laser cladding operations. Optics and Lasers in Engineering, 56, 113-120.

[25] Micali, M. K., & Dornfeld, D. (2016). Fully three-dimensional toolpath generation for point-based additive manufacturing systems. In Solid Freeform Fabrication Symposium (Vol. 27).

[26] Ding, D., Pan, Z., Cuiuri, D., Li, H., & Larkin, N. (2016). Adaptive path planning for wire-feed additive manufacturing using medial axis transformation. Journal of Cleaner Production, 133, 942-952.

[27] Choi, S. H., & Cheung, H. H. (2006). A topological hierarchy-based approach to toolpath planning for multi-material layered manufacturing. Computer-Aided Design, 38(2), 143-156.

[28] Jin, G. Q., Li, W. D., Tsai, C. F., & Wang, L. (2011). Adaptive tool-path generation of rapid prototyping for complex product models. Journal of manufacturing systems, 30(3), 154-164.

[29] Jin, Y. A., He, Y., & Fu, J. Z. (2013). An adaptive tool path generation for fused deposition modeling. In Advanced Materials Research (Vol. 819, pp. 7-12). Trans Tech Publications Ltd.

[30] Jin, Y. A., He, Y., Fu, J. Z., Gan, W. F., & Lin, Z. W. (2014). Optimization of tool-path generation for material extrusion-based additive manufacturing technology. Additive manufacturing, 1, 32-47.

[31] Wu, H., Xie, X., Liu, M., Chen, C., Liao, H., Zhang, Y., & Deng, S. (2020). A new approach to simulate coating thickness in cold spray. Surface and Coatings Technology, 382, 125151.

[32] Wu, H., Xie, X., Liu, M., Verdy, C., Zhang, Y., Liao, H., & Deng, S. (2020). Stable layer-building strategy to enhance cold-spray-based additive manufacturing. Additive Manufacturing, 35, 101356.

[33] Kennedy, J., & Eberhart, R. (1995, November). Particle swarm optimization. In Proceedings of ICNN'95-international conference on neural networks (Vol. 4, pp. 1942-1948). IEEE.

[34] Cichocka, J. M., Migalska, A., Browne, W. N., & Rodriguez, E. (2017, July). SILVEREYE–The implementation of particle swarm optimization algorithm in a design optimization tool. In International Conference on Computer-Aided Architectural Design Futures (pp. 151-169). Springer, Singapore.

[35] Lynch, M. E., Gu, W., El-Wardany, T., Hsu, A., Viens, D., Nardi, A., & Klecka, M. (2013). Design and topology/shape structural optimisation for additively manufactured cold sprayed components: This paper presents an additive manufactured cold spray component which is shape optimised to achieve 60% reduction in stress and 20% reduction in weight. Virtual and Physical Prototyping, 8(3), 213-231.